Modulation of the Intercalation Properties of Copper–Zinc Mixed-Metal Phosphonate Materials

Bouzid Menaa and Ian J. Shannon*[a]

Abstract: New layered mixed divalent metal vinylphosphonates $Cu^{II}_{1-x}Zn^{II}_{x}(O_3PC_2H_3)\cdot H_2O$ have been prepared from a range of pre-formed copper–zinc oxides $Cu^{II}_{1-x}Zn^{II}_{x}O$ obtained by isomorphous substitution of zinc into the tenorite-type structure of $Cu^{II}O$. The corresponding mixed divalent copper–zinc vinylphosphonates have been characterised by powder X-ray diffraction, elemental analysis, infrared spectroscopy and thermogravimetric analysis. All compounds have been shown to consist of a single-phase solid solution that crystallises in an monoclinic unit cell, space group $P2_1/c$ with $a = 9.86-9.90$, $b = 7.61-7.64$, $c = 7.32-7.35$ Å and $\beta = 95.9-96^\circ$, with the exception of the pure zinc vinylphosphonate ($x = 1$), the structure of which is comparable to other $Zn^{II}(O_3PR)\cdot H_2O$ materials. Studies of the intercalation of *n*-butylamine into the range of copper–zinc vinylphosphonates have demonstrated that significant modulation of the adsorption properties occurs; whereas one mole of amine is intercalated into the pure zinc vinylphosphonate to give $Zn^{II}(O_3PC_2H_3)\cdot(C_4H_9NH_2)$, for all other members of the series two moles of amine are coordinated to give intercalated compounds of composition $Cu^{II}_{1-x}Zn^{II}_{x}(O_3PC_2H_3)\cdot[(C_4H_9NH_2)_{1-x}(C_4H_9NH_2)_x]_2$ from which the amine can be sequentially removed from the different metal sites; this opens up possibilities for further applications of these materials.

Keywords: intercalations · layered compounds · metal phosphonates · organic–inorganic hybrid composites

Introduction

Layered metal phosphonate materials[1] have been the subject of increasing interest over the past few years. Following the early work in this area, which centred on the study of phosphates and phosphonates of tetravalent metals,[2–3] many more studies have been carried out that focus on the synthesis, crystal structures and properties of di-[4–8] and trivalent metals.[9, 10]

The synthesis of metal phosphonate materials may be carried out by a range of different preparation methods: by hydrothermal methods, co-precipitation in solution,[5, 11] organometallic routes[12] or by a melt method in which a solid mixture of metal hydroxide and phosphonic acid is heated in a sealed autoclave above the melting point temperature of the phosphonic acid used.[6]

These inorganic–organic hybrid compounds have many potential applications, owing to the large range of metals that can be used to form the inorganic backbone [$-MO_3P-$] and the range of organic groups (R) that may be attached to this backbone. The magnetic properties of materials containing metals such as copper or iron[13] have been investigated, and materials with phosphonates containing carboxylate/carboxylic acid[14, 15] sulfonate/sulfonic acid groups[16, 17] and/or amino[18] functionalities are of considerable interest for use as catalysts[19, 20] and ion exchangers.[21] The ability to intercalate species such as amines[22–24] or alcohols[25] into structures that contain a removable water molecule makes these materials suitable for use as sorbents[26] and in molecular recognition,[27] with further interest for building microporosity[28, 29] into these structures.

In our studies here, we have focused on divalent metal phosphonates $M^{II}(O_3PR)\cdot H_2O$, for which Cunningham et al.[30] first reported the synthesis of phenylphosphonate derivatives, and demonstrated the octahedral coordination of the metal (M = Mg, Cd, Zn, Co, Ni) from consideration of electronic spectra. Cao et al.[5] confirmed this sixfold coordination and reported for a homologous series of divalent metal phosphonates $M^{II}(O_3PR)\cdot H_2O$ (with M = Mg, Mn, Zn and R = alkyl) that all these layered compounds were isostructural, crystallising in an orthorhombic unit cell, space group $Pmn2_1$, with $a = 5.61-5.82$ and $c = 4.76-4.95$ Å, with the *b* cell parameter varying according to the size of the organic group. The octahedral coordination sphere around each metal centre is built up from four oxygen atoms shared with other metal atoms (two of these oxygen atoms coming from the

[a] Dr. I. J. Shannon, B. Menaa
School of Chemical Sciences
University of Birmingham
Birmingham, B15 2TT (UK)
Fax: (+44) 121-414-4403
E-mail: i.shannon@bham.ac.uk

0947-6539/02/0821-4884 $ 20.00+.50/0 *Chem. Eur. J.* **2002**, *8*, No. 21

same phosphonate group and chelating the metal centre) and a further unshared oxygen, which forms a direct link from the metal centre to only the phosphorus, and is completed by the oxygen of the water molecule.

Divalent copper phosphonates, $Cu^{II}(O_3PR)\cdot H_2O$,[31, 11] however, form a different structure, due most probably to the structure not being easily able to accommodate a Jahn–Teller distorted MO_6 octahedron. Clearfield et al.[31] determined the structure of the copper methyl- and phenylphosphonates and demonstrated that they are layered compounds containing copper atoms in an unusual five-coordinate distorted square-pyramidal environment. Each copper atom is bonded to four coplanar oxygen atoms (three phosphonate oxygens and one water oxygen), with a fifth Cu–O bond nearly perpendicular to the plane, completing the pentacoordination of the copper atoms. We recently solved the structures[32] of new materials that contain vinylphosphonate groups, $Cu^{II}(O_3PC_2H_3)\cdot H_2O$ and $Zn^{II}(O_3PC_2H_3)\cdot H_2O$. Although in both structures there are short contacts of approximately 4.15 Å between adjacent vinyl groups within the layers, the different metal coordination in these materials results in a change in the relative orientations of the vinyl groups, which may manifest itself in different reactivity towards topochemical reactions, such as solid-state [2+2] cyclodimerisation.[33, 34]

Most of the studies on divalent metal phosphonates have been carried out on systems that contain only one metal within the structure. In another recent paper,[35] we reported the first synthesis of mixed divalent metal phosphonate materials, $M^{II}_{1-x}M'^{II}_x(O_3PR)\cdot H_2O$, with (M, M′) = (Mg, Zn) and (Ni, Zn), and R = $-CH_3$, $-C_2H_3$, $-C_6H_5$ and $-(CH_2)_2COOH$. These were prepared by the melt method of synthesis,[6] by combining the corresponding mixed divalent metal hydroxides with different ratios of metal contents (x = 0, 0.1, 0.25, 0.5, 1) with the desired phosphonic acid. We found that both series of magnesium–zinc and nickel–zinc phosphonates have structures analogous to those of the pure divalent metal phosphonates $M^{II}(O_3PR)\cdot H_2O$ and that the metal cations were octahedrally coordinated in all cases. From ^{31}P solid-state MASNMR spectroscopy it could be seen that there was no ordering of the different metals within the structure, but also, importantly, no segregation of separate phases of the two different metal phosphonates was seen.

We have extended our studies to investigation of other combinations of divalent metals in metal phosphonate materials, and present here the results of our work on mixed copper–zinc vinylphosphonates—$Cu^{II}_{1-x}Zn^{II}_x(O_3PC_2H_3)\cdot H_2O$—in which we expected modulation of properties on account of the different structures adopted by pure zinc phosphonates and copper phosphonates described above.

Materials such as those prepared here, containing two different metals, could enable the tuning of ion-exchange and proton conduction properties (with appropriate R-group functionality) and adsorption properties, and have further possibilities for modification to generate much sought-after regular porous structures, on account of differing exchange properties at each metal site.

We have focused here on the intercalation reaction of alkylamines into these materials, on account of the known differences in the behaviour of copper[24] and zinc[36, 37] phosphonates. Initial dehydration of $Cu^{II}(O_3PR)\cdot H_2O$ and $Zn^{II}(O_3PR)\cdot H_2O$ (R = –Me, –Ph) leads to different structures. While the dehydrated copper compounds show an increase in the interlayer spacing of approximately 1 Å (involving a structural rearrangement unique to copper metals), the layer spacing in anhydrous zinc phenylphosphonate[37] does not change significantly (due to the size of the phenyl group) and dehydrated zinc methylphosphonate shows a decrease in interlayer distance,[36] suggested to be due to another rearrangement leading to a fourfold coordination of the zinc in the anhydrous compound.

This dehydration step creates open coordination sites favourable for amine intercalation; variation in the interlayer distance is observed depending on the size and the shape of the amine intercalated. Cao and Mallouk[23] studied the intercalation of zinc methylphosphonate with a range of alkylamines $C_nH_{2n+2}NH_2$. Intercalation with *n*-butylamine was characterised by an expansion of the interlayer distance from 8.7 Å for the hydrated compounds to 13.64 Å for the intercalated zinc methylphosphonate. Poojary and Clearfield[22] determined the structure of $Zn^{II}(O_3PC_6H_5)\cdot R'NH_2$ (R′ = C_3H_7, C_4H_9, C_5H_{11}), the structure of which rearranges upon intercalation leading to tetrahedral zinc atoms coordinated by three phosphonate oxygen atoms and one nitrogen atom. In parallel, Bujoli et al.[38] confirmed this fourfold coordination, on the basis of EXAFS-XANES measurements, for the intercalated zinc alkylphosphonates. Studies on copper methyl- and phenylphosphonates showed the absorption of one mole of *n*-butylamine and two moles of *n*-butylamine, respectively, with an increase in the interlayer spacing to 14.8 Å observed for both.

Below, we present the results of our studies on the intercalation of *n*-butylamine within the mixed copper–zinc vinylphosphonates $Cu^{II}_{1-x}Zn^{II}_x(O_3PC_2H_3)\cdot H_2O$, and show that we do indeed see unusual behaviour on account of the structural modulations induced in these materials—a result which demonstrates the potential for tuning these types of material for specific application through control of the metal cation ratio in the structure.

Results and Discussion

Mixed divalent copper–zinc oxides: The copper–zinc oxides $Cu^{II}_{1-x}Zn^{II}_xO$ to be used as precursors for the synthesis of the corresponding vinylphosphonates were prepared in the same manner as we had previously used to prepare oxides and hydroxides.[35] The powder X-ray diffraction patterns (Figure 1) recorded at ambient temperature show the success of the isomorphous substitution of Zn^{II} into the tenorite structure of $Cu^{II}O$, with the samples of $Cu^{II}_{1-x}Zn^{II}_xO$ ($x \neq 1$) becoming more brown in colour as the zinc content increased. Indexing showed that for x = 0, 0.1, 0.25, 0.5, $Cu^{II}_{1-x}Zn^{II}_xO$ crystallises in a monoclinic space group $C2/c$, with a = 5.10–5.15, b = 3.38–3.43, c = 4.70–4.71 Å, β = 99.33–99.81° (details of cell parameters are given in Table 1). In contrast, $Zn^{II}O$ (x = 1), in its zincite form is hexagonal, space group $P6_3mc$, with $a = b$ = 3.26 and c = 5.22 Å.

  0947-6539/02/0821-4885 $ 20.00+.50/0

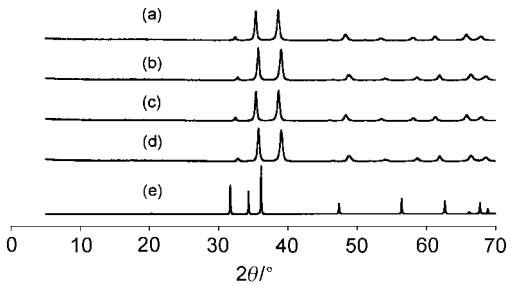

Figure 1. Powder X-ray diffraction patterns for $Cu^{II}_{1-x}Zn^{II}_{x}O$: a) $x=0$, b) $x=0.1$, c) $x=0.5$, d) $x=0.5$, e) $x=1$.

Table 1. Unit cell parameters for $Cu^{II}_{1-x}Zn^{II}_{x}O$ for $x=0$, 0.1, 0.25, 0.5, 1.

$Cu_{1-x}Zn_xO$	Symmetry	Cell Parameters			
		a [Å]	b [Å]	c [Å]	β [°]
$x=0$	monoclinic	5.14	3.43	4.71	99.33
$x=0.1$	space group $C2/c$	5.15	3.42	4.71	99.76
$x=0.25$		5.14	3.41	4.71	99.81
$x=0.5$		5.10	3.38	4.70	99.79
$x=1$	hexagonal space group $P6_3mc$	3.26	3.26	5.22	–

Attempts to synthesise single-phase copper–zinc oxides with a higher zinc content ($x>0.5$ and $x\neq1$) were unsuccessful, instead a mixture of phases composed of the zincite and the tenorite structures resulted. While one might consider the use of a physical mixture of the two different oxides in an attempt to obtain phosphonates with $x>0.5$, this procedure would more probably lead to a mixture of the phosphonate materials, owing to the nonintimate interaction between oxides.

Mixed divalent copper–zinc vinylphosphonates: For the different Cu:Zn ratios used, the X-ray diffraction patterns of the mixed metal phosphonates $Cu^{II}_{1-x}Zn^{II}_{x}(O_3PC_2H_3)\cdot H_2O$ (with $x=0$, 0.1, 0.25, 0.5) showed a crystalline single phase characterised by the absence of any unreacted copper–zinc oxides (Figure 2). On the basis of the X-ray patterns, the whole range (except for $x=1$) has the same structure as pure copper vinylphosphonate, indicating that the zinc can isomorphously replace copper in the copper vinylphosphonate structure.

The $Cu^{II}_{1-x}Zn^{II}_{x}(O_3PC_2H_3)\cdot H_2O$ materials (with $x=0$, 0.1, 0.25, 0.5) have all been indexed on the basis of a monoclinic unit cell, space group $P2_1/c$, with $a=9.86-9.90$, $b=7.61-7.64$, $c=7.32-7.35$ Å and $\beta=95.9-96^\circ$ (Table 2). In contrast, the structure of the pure zinc vinylphosphonate differs from the copper structure (Figure 2e): $Zn^{II}(O_3PC_2H_3)\cdot H_2O$ crystallises in an orthorhombic unit cell, space group $Pmn2_1$, with $a=5.68$, $b=9.83$ and $c=4.80$ Å. The a and c cell parameters are similar to those observed for other zinc phosphonates ($Zn^{II}(O_3PR)\cdot H_2O$, R = –Me, –Ph),[36, 37] with b approximately corresponding to the interlayer distance and of the size expected for the size of the vinyl group. No evidence for any segregation of an impurity of zinc vinylphosphonate is seen in the patterns for the mixed copper–zinc vinylphosphonates.

Table 2. Unit cell parameters for $Cu^{II}_{1-x}Zn^{II}_{x}(O_3PC_2H_3)\cdot H_2O$ for $x=0$, 0.1, 0.25, 0.5, 1.

$Cu_{1-x}Zn_x(O_3PC_2H_3)\cdot H_2O$	Symmetry	Cell Parameters			
		a [Å]	b [Å]	c [Å]	β [°]
$x=0$	monoclinic	9.88	7.63	7.33	96.01
$x=0.1$	space group $P2_1/c$	9.86	7.61	7.32	95.95
$x=0.25$		9.90	7.64	7.35	95.93
$x=0.5$		9.89	7.64	7.32	95.90
$x=1$	orthorhombic space group $Pmn2_1$	5.68	9.83	4.80	–

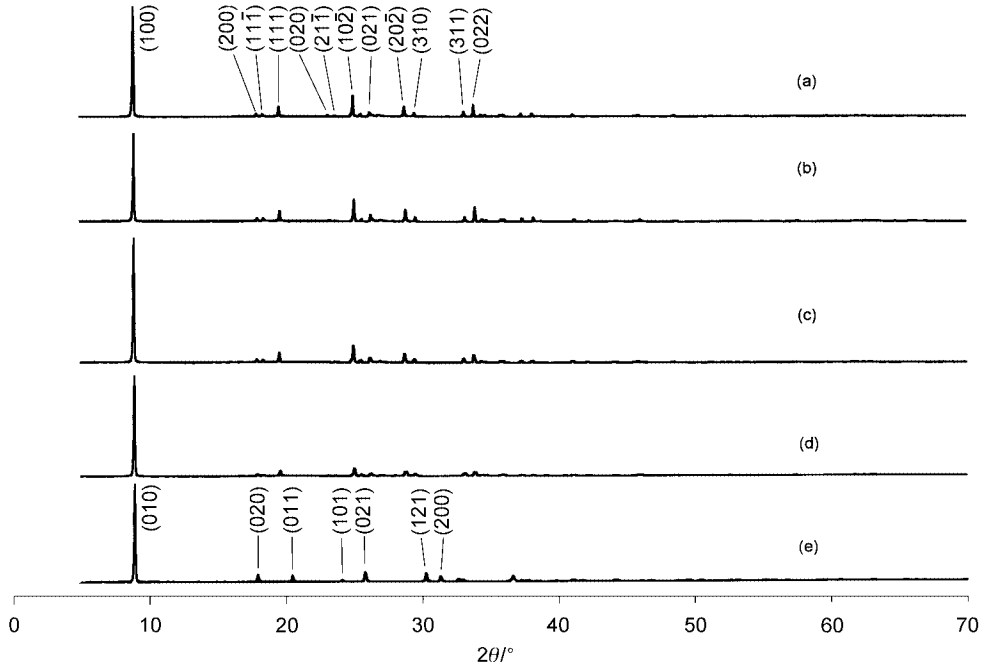

Figure 2. Powder X-ray diffraction patterns for $Cu^{II}_{1-x}Zn^{II}_{x}(O_3PC_2H_3)\cdot H_2O$: a) $x=0$, b) $x=0.1$, c) $x=0.5$, d) $x=0.5$, e) $x=1$. The peak indices labelled in a) apply to patterns a)–d), which show that all four structures are isostructural with $Cu^{II}(O_3PC_2H_3)\cdot H_2O$, while $Zn^{II}(O_3PC_2H_3)\cdot H_2O$ has a different structure (as described in the text), and so the indexing for pattern e) is different.

0947-6539/02/0821-4886 $ 20.00+.50/0 *Chem. Eur. J.* **2002**, *8*, No. 21

The infrared spectrum for $Cu^{II}(O_3PC_2H_3)\cdot H_2O$ (Figure 3a) shows two well-separated, strong bands (−OH stretching modes at 3260 and 3030 cm^{-1}) and a medium strength band at 1573 cm^{-1} attributed to the −OH bending modes. The three strong bands at 1093, 1041 and 1030 cm^{-1} are associated with

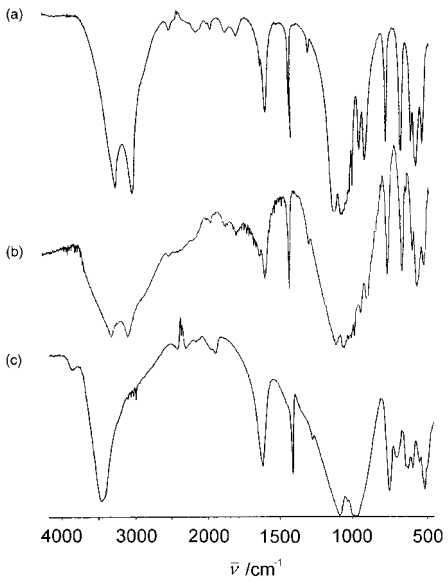

Figure 3. FTIR spectra for $Cu^{II}_{1-x}Zn^{II}_x(O_3PC_2H_3)\cdot H_2O$: a) $x=0$, b) $x=0.5$, c) $x=1$.

the PO_3 stretching modes. These features are similar to those observed for other copper phosphonates (−Me, −Ph, −Et), and further confirm the structural similarities between copper vinylphosphonate and the other known copper phosphonates.

For $Zn^{II}(O_3PC_2H_3)\cdot H_2O$, the infrared spectrum is clearly different (Figure 3c), and shows similar bands to the structurally analogous $M^{II}O_3PR\cdot H_2O$ (M = Mn, Mg, Zn, Ni, Co, Cd)[5, 6, 39] containing alkyl, aryl or phenyl groups. A strong sharp band at 3456 cm^{-1} is attributed to the stretching vibrations of the OH from the water molecule coordinated to the metal, with the corresponding deformation band occurring at 1617 cm^{-1}. Bands in the 1089–974 cm^{-1} region are associated with the P−O vibration of the PO_3 group, and four small stretching bands at 2973, 3008, 3030 and 3075 cm^{-1} corresponding to the vinylic −CH vibrations.

The infrared data for the mixed copper–zinc materials (shown for $x=0.5$ in Figure 3c) are all qualitatively similar to those for the pure copper phosphonate, reinforcing the evidence from the above XRD data that the zinc substitutes into the copper vinylphosphonate structure.

Dehydration and intercalation of $Cu^{II}_{1-x}Zn^{II}_x(O_3PC_2H_3)\cdot H_2O$ with *n*-butylamine

Dehydrated copper–zinc vinylphosphonates, $Cu^{II}_{1-x}Zn^{II}_x(O_3PC_2H_3)$: Copper vinylphosphonate monohydrate, $Cu^{II}(O_3PC_2H_3)\cdot H_2O$, and its analogous copper–zinc vinylphosphonates, $Cu^{II}_{1-x}Zn^{II}_x(O_3PC_2H_3)\cdot H_2O$ ($x=0.1$, 0.25, 0.5, $x\neq 1$), begin to lose their water molecule around 135–140 °C (Figure 4). The onset temperature for loss of the vinyl group, at 300 °C, is very low compared with other metal phosphonate

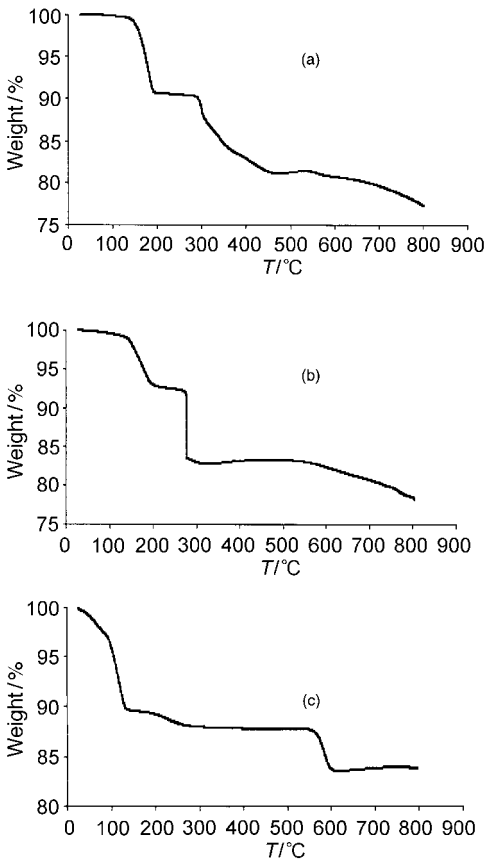

Figure 4. TGA curves for $Cu^{II}_{1-x}Zn^{II}_x(O_3PC_2H_3)\cdot H_2O$: a) $x=0$, b) $x=0.5$, c) $x=1$.

materials $M^{II}O_3PR\cdot H_2O$, and particularly compared with the zinc vinylphosphonate, for which the dehydration step occurs at lower temperature (80 °C), but the vinyl group remains intact up to approximately 560 °C. This suggests that the copper phosphonates, and copper vinylphosphonate in particular, are stable in the hydrated phase but very unstable upon dehydration, when compared with compounds such as $Mg^{II}(O_3PC_2H_3)\cdot H_2O$ and $Zn^{II}(O_3PC_2H_3)\cdot H_2O$. Such instability of copper phosphonate materials upon dehydration has also been reported for $Cu^{II}(O_3PCH_3)\cdot H_2O$ and $Cu^{II}(O_3PC_6H_5)\cdot H_2O$,[31] which lose their coordinated water at around 190 °C and 160 °C, respectively, and their organic components at around 370 °C.

The mixed copper–zinc vinylphosphonate (Figure 4b) exhibit the same behaviour as the pure copper vinylphosphonate upon dehydration. It is important to note at this stage that on dehydration of mixed copper–zinc vinylphosphonates we do not see two discrete weight losses corresponding to removal of the water molecule coordinated to the zinc metals and the copper metals, respectively, but only a single step in the TGA trace. The temperature at which the vinyl group is lost is close to that for the pure copper vinylphosphonate, again providing evidence that the zinc is isomorphously substituting for copper in the structure.

The solid residue from the pure zinc vinylphosphonate has been identified by XRD as the zinc pyrophosphate $Zn_2P_2O_7$, and although it could not be confirmed it is to be expected

  0947-6539/02/0821-4887 $ 20.00+.50/0

that the product from starting with copper vinylphosphonate should be a copper pyrophosphate phase.

On the basis of their powder X-ray patterns (Figure 5), the anhydrous copper, zinc and mixed copper–zinc vinylphosphonates are found to be poorly crystalline, although the retention of a layered structure is apparent and an indication

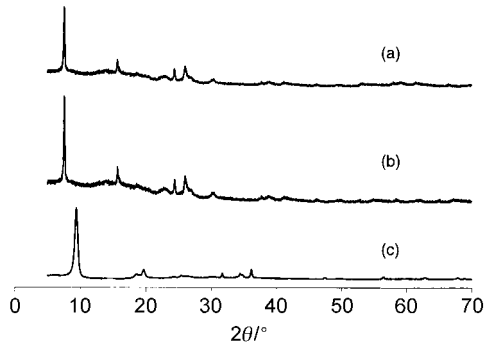

Figure 5. Powder X-ray diffraction patterns recorded at 180 °C for $Cu^{II}_{1-x}Zn^{II}_{x}(O_3PC_2H_3)$: a) $x = 0$, b) $x = 0.5$, c) $x = 1$.

of the interlayer spacing can be obtained from the first strong reflection. Once again, evidence can be seen for the dehydrated mixed copper–zinc vinylphosphonates $Cu^{II}_{1-x}Zn^{II}_{x}(O_3PC_2H_3)$, ($x = 0.1$, 0.25, 0.5, $x \neq 1$) behaving in the same manner as the pure copper vinylphosphonate $Cu^{II}(O_3PC_2H_3)$.

The interlayer distance decreases upon dehydration from 9.83 to 9.48 Å for the zinc vinylphosphonate, whereas an increase is observed for the copper vinylphosphonate from 9.84 to 10.37 Å and from 9.90 to approximately 10.4 Å for all the mixed copper–zinc vinylphosphonates.

The increase in the interlayer distance for the copper and copper–zinc vinylphosphonates can be explained by the same structural rearrangement as reported by Zhang et al.[24] and Bujoli et al.[11] for copper methyl-, phenyl- and ethylphosphonate, and is believed to be a reversible structural rearrangement unique to copper phosphonates on dehydration. Bujoli et al. explained that dehydration of the copper ethylphosphonate results in the shift of one of the phosphonate oxygens to occupy the vacant coordination site after water removal. In other words, while in the hydrated phase only one of the phosphonate oxygen atoms bridges between two copper atoms, after dehydration a second oxygen atom also takes up this configuration situation. This reorganisation of the layer induces a decrease in the lattice parameter along the *b* axis from 7.3 to 5.7 Å, and the resulting distortion of the structure also leads to an interlayer spacing increase from 9.92 to 10.78 Å. The rearrangement occurs in order to retain the copper atom as a five-coordinate site rather than the highly unfavourable (highly distorted tetrahedral) coordination that would result from dehydration without rearrangement.

$Zn^{II}(O_3PC_2H_3)$ shows the same behaviour as seen for other $Zn^{II}(O_3PR)$ compounds, with a decrease in the interlayer distance. Whereas one might expect that dehydration would result only in a reduction in coordination number to five but without change in the bonding within the layers, Bujoli et al.[36] have instead shown for $Zn^{II}(O_3PCH_3)$ that the reduction in *d*-spacing is a result both of a rearrangement between layers caused by a translation of the layers, resulting in the methyl groups of one layer nestling in the space vacated by the water molecule from the adjacent layer, and also of the zinc atoms taking a tetrahedral geometry. This tetrahedral geometry arises from four oxygen atoms from three different phosphonate groups which adopt a (112) connectivity due to the two phosphonate oxygen atoms that were initially bridging two zinc atoms becoming singly bonded to the metal atoms, while the connectivity of the third oxygen changes from 1 to 2. While we cannot confirm this explicitly from our X-ray patterns of $Zn^{II}(O_3PC_2H_3)$ (Figure 5c), it is likely that the same rearrangement occurs for our compounds.

Upon immersion of the dehydrated copper, copper–zinc and zinc vinylphosphonates in distilled water the structures revert to their monohydrate phases, as evidenced by the X-ray powder patterns, demonstrating the reversibility of the (de)hydration process.

Intercalation of n-*butylamine into* $Cu^{II}_{1-x}Zn^{II}_{x}(O_3PC_2H_3)$: Several *n*-butylamine-intercalated species $Cu^{II}_{1-x}Zn^{II}_{x}(O_3PC_2H_3)$ ($x = 0$, 0.1, 0.25, 0.5, 1) have been characterised by powder X-ray diffraction. The patterns for all the compounds (Figure 6) show, as expected, an increase in the

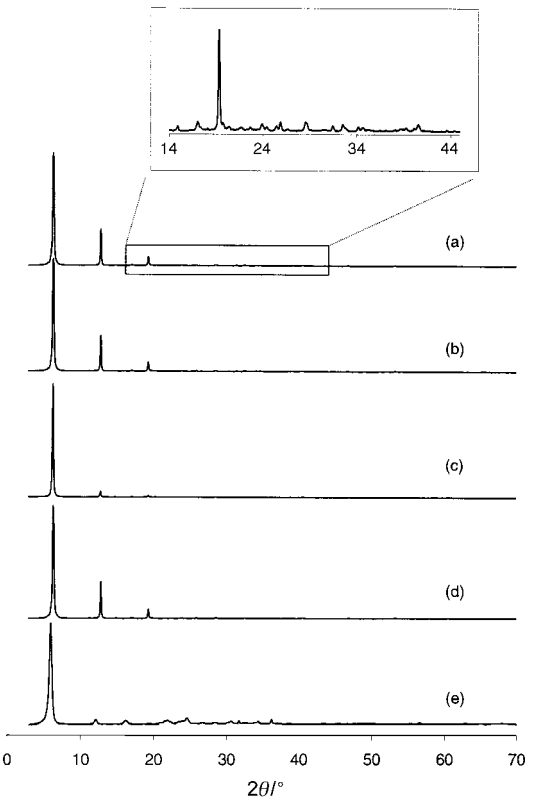

Figure 6. Powder X-ray diffraction patterns for: a) $Cu^{II}(O_3PC_2H_3)\cdot(C_4H_9NH_2)_2$, b) $Cu^{II}_{0.5}Zn^{II}_{0.5}(O_3PC_2H_3)\cdot[(C_4H_9NH_2)_{0.5}(C_4H_9NH_2)_{0.5}]_2$, c) $Zn^{II}(O_3PC_2H_3)\cdot(C_4H_9NH_2)$.

interlayer distance according to the length of the alkyl chain within the *n*-butylamine. The absence of any peaks characteristic of the dehydrated starting material confirms that full intercalation has occurred. The interlayer distance increases from 9.83 Å for the hydrated phase to 14.88 Å for the

0947-6539/02/0821-4888 $ 20.00+.50/0 *Chem. Eur. J.* **2002**, *8*, No. 21

intercalated phase of the zinc vinylphosphonate, and from 9.88 to 13.6 Å and from 9.8–9.9 to 13.9 Å for the pure copper and the mixed copper–zinc vinylphosphonates, respectively. As one would expect from the differences observed for the dehydrated phases, the structure of amine-intercalated zinc vinylphosphonate is different from that of the intercalated pure copper and mixed copper–zinc vinylphosphonates. Again, the pure copper and mixed copper–zinc phosphonates behave in the same manner.

The X-ray pattern for zinc vinylphosphonate was indexed on an orthorhombic unit cell, $a = 14.99$, $b = 8.53$, $c = 8.44$ Å, but the powdered sample was not crystalline enough for structural determination. By way of comparison, the structure of $Zn^{II}(O_3PC_6H_5)\cdot C_4H_9NH_2$ (monoclinic, space group $P2_1/c$, $a = 14.69$, $b = 8.95$, $c = 9.71$ Å, $\beta = 102.46^\circ$) is known,[22] and shows fourfold coordination of the zinc metal atoms; this is accomplished by a further rearrangement keyed by the contact with the amine and leads to the formation of larger open rings containing four zinc atoms coordinated to three phosphonate oxygen atoms and one nitrogen atom.

IR data (Figure 7) also provide strong evidence of the amine coordination to the copper and zinc in the mixed divalent copper–zinc vinylphosphonates. The characteristic

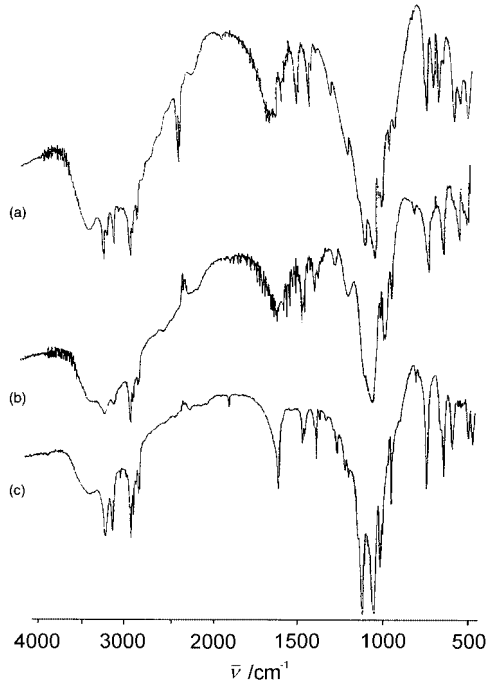

Figure 7. FTIR spectra for: a) $Cu^{II}(O_3PC_2H_3)\cdot(C_4H_9NH_2)_2$, b) $Cu^{II}_{0.5}Zn^{II}_{0.5}(O_3PC_2H_3)\cdot[(C_4H_9NH_2)_{0.5}(C_4H_9NH_2)_{0.5}]_2$, c) $Zn^{II}(O_3PC_2H_3)\cdot(C_4H_9NH_2)$.

O–H stretching bands (3260 and 3030 cm^{-1}) and the deformation band at about 1573 cm^{-1} of coordinated water for $Cu^{II}(O_3PC_2H_3)\cdot H_2O$ and $Cu^{II}_{1-x}Zn^{II}_x(O_3PC_2H_3)\cdot H_2O$ ($x \neq 1$) are absent in the intercalated compounds (although some water is present due to the hygroscopic nature of the KBr discs). Instead, we observe three sharper bands around 3260, 3225 and 3141 cm^{-1}, attributable to the NH stretching of the amine coordinated to the metals, and a deformation band at 1637 cm^{-1}. The stretching bands of the methylene ($-CH_2-$) groups of the *n*-butylamine appear in the 2960–2870 cm^{-1} region. The bands representing the PO_3 vibrations occur between 1190 and 944 cm^{-1} and indicate that the basic structure is retained after amine intercalation. The IR spectra of the *n*-butylamine-intercalated mixed divalent copper–zinc vinylphosphonates (e.g., $x = 0.5$, Figure 7b) and the pure copper vinylphosphonate (Figure 7a) are almost superimposable, confirming that both have similar structures.

In the case of the zinc vinylphosphonate intercalated with *n*-$C_4H_9NH_2$, the spectra are qualitatively the same as that of $Zn^{II}(O_3PCH_3)\cdot C_4H_9NH_2$,[36] with similar PO_3 vibrations at 1120 (s), 1054 (s) and 1002 (s) cm^{-1}, suggesting that both compounds have the same arrangement within the layers and the same fourfold coordination for the zinc metals. The OH stretch vibrations of the water molecule of the hydrated phase are also replaced by three sharper bands at 3245, 3165 and 3075 cm^{-1}, attributable to the NH stretch, with the corresponding deformation band at 1615 cm^{-1}, and the methylene group stretches around the 2960–2870 cm^{-1} region.

Because of the paramagnetic nature of the copper nuclei, it was only possible to record ^{31}P solid-state MASNMR spectra for the zinc vinylphosphonate monohydrate (Figure 8a) and the intercalated zinc vinylphosphonate with *n*-butylamine

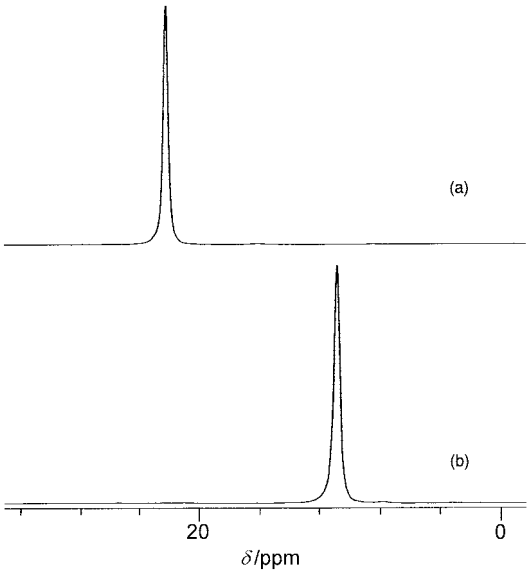

Figure 8. ^{31}P solid-state MASNMR spectra for: a) $Zn^{II}(O_3PC_2H_3)\cdot H_2O$ and b) $Zn^{II}(O_3PC_2H_3)\cdot(C_4H_9NH_2)$.

(Figure 8b), each of these showing a single resonance. The unique peak observed at $\delta = 21.86$ ppm for the hydrated phase and at $\delta = 11.11$ ppm for its intercalate is indicative of both chemical and structural homogeneity in the material, with the difference between the chemical shift observed for the hydrated compound and that for the *n*-butylamine intercalated compound reflecting the environmental change around the phosphorus atoms.

Thermogravimetric analysis (Figure 9) gives us information about the stability and the stoichiometry of the intercalated compounds, and has revealed some surprising results.

  0947-6539/02/0821-4889 $ 20.00+.50/0

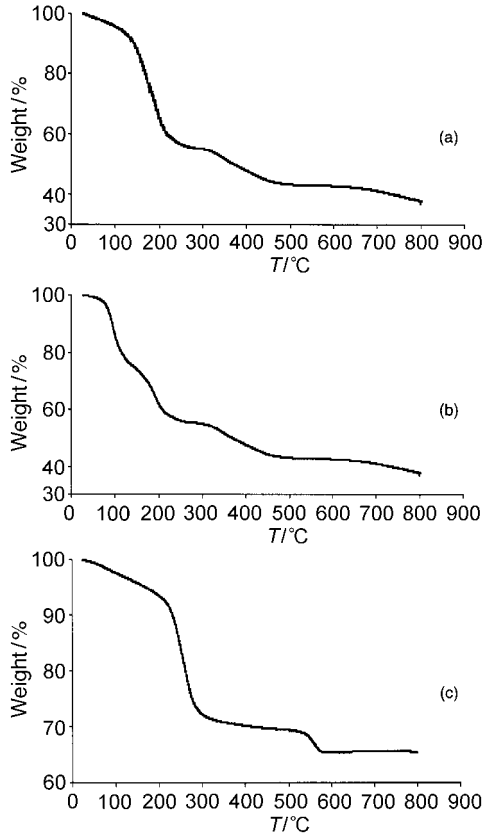

Figure 9. TGA curves for: a) $Cu^{II}(O_3PC_2H_3)\cdot(C_4H_9NH_2)_2$, b) $Cu^{II}_{0.5}Zn^{II}_{0.5}(O_3PC_2H_3)\cdot[(C_4H_9NH_2)_{0.5}(C_4H_9NH_2)_{0.5}]_2$, c) $Zn^{II}(O_3PC_2H_3)\cdot(C_4H_9NH_2)$.

The TGA curve of the copper vinylphosphonate intercalated with the *n*-butylamine (Figure 9a) shows two main regions of weight loss. The first loss of mass is attributable to the removal of the *n*-butylamine, commencing at approximately 80 °C and proceeding in one clear step up to around 280 °C. The experimental weight loss of 46.27 % is in excellent agreement with a theoretical weight loss of 46.2 % corresponding to two moles of amine having been absorbed. This is comparable with copper phenylphosphonate, in which two moles of amine are also adsorbed, but is different to copper methylphosphonate, in which only one mole is absorbed. Sixfold coordination would then be expected, with the intercalation of two moles of amines in the dehydrated copper vinylphosphonates. A further weight loss beginning at around 310–320 °C is attributable to the removal of the vinylic group, and this low temperature again indicates the instability of the compound upon deamination. To summarise, on the basis of the thermogravimetric analysis the intercalated copper vinylphosphonate has the stoichiometry $Cu^{II}(O_3PC_2H_3)\cdot(C_4H_9NH_2)_2$.

For the *n*-butylamine-intercalated zinc vinylphosphonate, the deamination occurs in a clear one-step process starting at a higher temperature (200 °C), indicating much greater stability of the intercalated compound. In this instance, however, the percentage weight loss of the amine (22.7 %) is in good agreement with only one mole of *n*-butylamine being absorbed. The weight loss corresponding to removal of the vinyl group occurs around 530 °C; this is consistent with that seen for other amine-intercalated zinc phosphonate structures in the literature.[22]

The most interesting behaviour, however, is observed for the mixed copper–zinc vinylphosphonate intercalated with the *n*-butylamine, for which two distinct weight losses attributed to the removal of the amine are observed. (Note that this is in direct contrast to the TGA results for the hydrated complexes, for which only one step was seen for water removal irrespective of the Cu:Zn ratio). The experimental percentage weight loss (46 %) corresponds to two moles of *n*-butylamine and, for the data shown for the removal of the amine from the $Cu^{II}_{0.5}Zn^{II}_{0.5}(O_3PC_2H_3)$ intercalated compound (Figure 9b), we can see that this is split into two equal steps (of 23 %) corresponding first to the removal of amine coordinated to copper (commencing at 80 °C) followed by removal of the second mole of amine coordinated to the zinc sites (commencing at 130 °C). For the other mixed copper–zinc vinylphosphonates studied, the relative magnitude of the percentage weight losses for these two steps varies in direct proportion to the ratio of copper to zinc present in the structure (Table 3). Thus we can write the general formula of these compounds as: $Cu^{II}_{1-x}Zn^{II}_{x}(O_3PC_2H_3)\cdot[(C_4H_9NH_2)_{1-x}(C_4H_9NH_2)_x]_2$ (for $x \neq 1$). (Note that in this nomenclature $(C_4H_9NH_2)_{1-x}$ refers to the amine coordinated to the copper atoms and $(C_4H_9NH_2)_x$ to that coordinated to the zinc atoms.) The further mass loss, which begins at 310 °C, is attributed to removal of the vinyl group.

It is worth noting that intercalation was complete within two days for the zinc vinylphosphonate, whereas full intercalation needed a longer time (a week) for the pure copper vinylphosphonate and the mixed copper–zinc vinylphosphonates. This is attributable to the more stable open structure for the intercalation of the zinc vinylphosphonate. Greater rearrangement may also occur during the intercalation process for the copper and mixed copper–zinc vinylphosphonate compounds, in which two moles of amine are required to be intercalated.

Because of the poor crystallinity of the $Cu^{II}_{1-x}Zn^{II}_{x}(O_3PC_2H_3)\cdot[(C_4H_9NH_2)_{1-x}(C_4H_9NH_2)_x]_2$ samples (e.g., $x = 0$, 0.5, Figure 10a–c), we have not yet been possible to pin down

Table 3. Weight loss percentages for the removal of *n*-butylamine from $Cu^{II}_{1-x}Zn^{II}_{x}(O_3PC_2H_3)\cdot[(C_4H_9NH_2)_{1-x}(C_4H_9NH_2)_x]_2$ with $x = 0$, 0.1, 0.25 and 0.5, and $Zn^{II}(O_3PC_2H_3)\cdot(C_4H_9NH_2)$.

$Cu_{1-x}Zn_x(O_3PC_2H_3)\cdot(C_4H_9NH_2)_n$		Weight loss		Weight loss	$T_{initial} - T_{final}$ [°C]
x	n	expected [%] ($-C_4H_9NH_2$)		found [%]	
0	2	46.27		46.20	80–280
0.1	2	46.24	41.61	38.12	80–131/134
			4.62	6.38	134–265
0.25	2	46.20	34.65	31.27	85–135
			11.55	13.45	135–270
0.5	2	46.13	23.06	21.15	80–130
			23.06	21.15	130–280
1	1	22.97		22.72	215–420

0947-6539/02/0821-4890 $ 20.00+.50/0 *Chem. Eur. J.* **2002**, *8*, No. 21

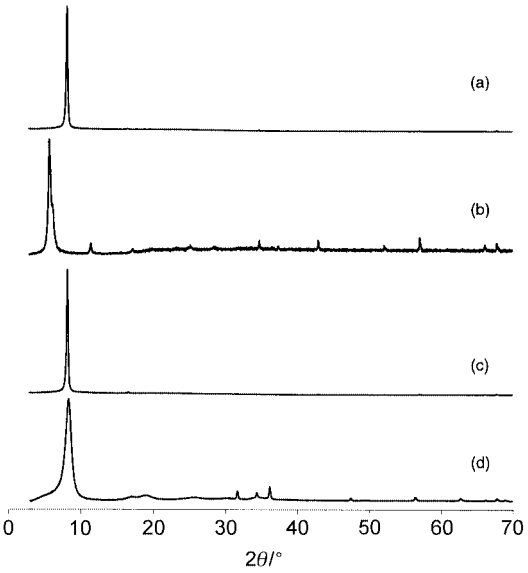

Figure 10. Powder X-ray diffraction patterns recorded at high temperature for: a) $Cu^{II}(O_3PC_2H_3)\cdot(C_4H_9NH_2)_2$ at 280 °C, b) $Cu^{II}_{0.5}Zn^{II}_{0.5}(O_3PC_2H_3)\cdot[(C_4H_9NH_2)_{0.5}(C_4H_9NH_2)_{0.5}]_2$ at 130 °C, c) $Cu^{II}_{0.5}Zn^{II}_{0.5}(O_3PC_2H_3)\cdot[(C_4H_9NH_2)_{0.5}(C_4H_9NH_2)_{0.5}]_2$ at 280 °C, d) $Zn^{II}(O_3PC_2H_3)\cdot(C_4H_9NH_2)$ at 300 °C.

any clear structural information regarding the coordination of the metals at the intermediate stages during the deamination process. For the sample with $x = 0.5$, the first reflection in the powder XRD pattern, however, does show an increase in the interlayer distance from 13.9 Å for the intercalated compound to 15.1–15.3 Å at the end of the first weight loss (130 °C); this suggests a rearrangement of the environment around the copper atoms, similar to that observed on dehydration, after removal of the amine coordinated to copper. However, upon full removal of the amine from all samples, we do not obtain the same XRD pattern as for the dehydrated phase; this suggests a nonreversible process between the amine-intercalated compound and the dehydrated phase.

For $Zn^{II}(O_3PC_2H_3)\cdot(C_4H_9NH_2)$, deamination showed a decrease in the interlayer distance from 14.88 to 10.49 Å (Figure 10d), again different from the dehydrated phase of zinc vinylphosphonate (9.43 Å), and once again giving evidence of the non-topotacticity between the deaminated and the dehydrated compound.

Conclusion

We have shown in this paper that we can obtain copper vinylphosphonate and zinc vinylphosphonate by the melt synthesis method with metal oxides as precursors. The isomorphous substitution of zinc into the $Cu^{II}O$ tenorite-type structure leads to a range of copper–zinc oxides, $Cu^{II}_{1-x}Zn^{II}_xO$ (with $x = 0.1, 0.25, 0.5$), suitable for the preparation of the corresponding new mixed copper–zinc vinylphosphonates, $Cu^{II}_{1-x}Zn^{II}_x(O_3PC_2H_3)\cdot H_2O$, with the same structural characteristics as pure copper vinylphosphonate.

Our aim in this work was to investigate how the incorporation of two different metals within a single metal phosphonate structure could be used to modulate the properties of these materials, and this has been strikingly illustrated through the amine intercalation studies undertaken. Whereas only one mole of amine is intercalated into the zinc vinylphosphonate, two moles intercalate the copper and the mixed copper–zinc vinylphosphonates. Moreover, in the mixed copper–zinc vinylphosphonates, the deamination process occurs in two steps directly proportional in size to the Cu:Zn ratio (i.e., if we write the general formula for these materials as $Cu^{II}_{1-x}Zn^{II}_x(O_3PC_2H_3)\cdot[(C_4H_9NH_2)_{1-x}(C_4H_9NH_2)_x]_2$, then we lose $2(1-x)$ moles of *n*-butylamine coordinated to the copper during the first step and $2x$ moles of *n*-butylamine coordinated to the zinc during the second step.

This has important consequences as regards the potential applications of such systems. One can envisage this method as a route to tuneable porous structures through variation of the ratio of metals present and the nature of the amine (or other intercalate), combined with the control we have over the conditions for partial removal of the intercalated species. Projected uses for such materials are envisaged in molecular recognition and selective sorption processes. Alternatively, the work presented here also provides a route to selective binding of different species to the two different metal sites; this could facilitate stereoregular reactions (e.g., polymerisations, cycloadditions) to be carried out within the constrained interlayer environment.

Experimental Section

Starting materials: Chemicals used were of reagent grade quality and were obtained from commercial sources. Zinc nitrate hexahydrate and copper(II) nitrate hemipentahydrate were purchased from Avocado. Vinylphosphonic acid and *n*-butylamine (99%), from Aldrich, were used without further purification.

Characterisation: Powder X-ray diffraction patterns were recorded for the copper–zinc oxides and copper–zinc vinylphosphonate monohydrates at room temperature with $Cu_{K\alpha1}$ radiation ($\lambda = 1.54056$ Å) on a Siemens D5000 diffractometer, operating in transmission mode with a primary Ge monochromator. X-ray data were collected at high temperature to record the patterns of the dehydrated compounds and the intercalated copper–zinc vinylphosphonates upon the deamination steps with a Siemens D5005 diffractometer with $Cu_{K\alpha1} + Cu_{K\alpha2}$ radiation ($\lambda = 1.5418$ Å) and operating with a Gobel mirror. Indexing of the data was carried out with the packaged programs.

FTIR spectra were recorded as KBr pellets on a Perkin–Elmer Paragon 1000 FTIR spectrometer at a spectral resolution of 4 cm^{-1}.

Thermogravimetric analysis was carried out on a Perkin–Elmer TGA6 instrument. Samples, in an alumina crucible, were heated at a rate of 10 °C min^{-1} from 25 °C to a maximum of 800 °C in an atmosphere of flowing nitrogen (20 mL min^{-1}).

^{31}P solid-state MASNMR spectra were recorded for the pure zinc vinylphosphonate monohydrate and its intercalate with *n*-butylamine ($Zn^{II}O_3PC_2H_3\cdot C_4H_9NH_2$) on a Chemagnetics CMX Infinity 300 spectrometer with a 3.2 mm double resonance probe. The standard cross-polarisation pulse sequence was used with a contact time of 6.0 ms, a recycle delay of typically 15.0 s, a spinning frequency of 7 kHz ± 2 Hz and a ^1H decoupling field strength of approximately 100 kHz. The spectra are referenced to phosphoric acid (85% by weight) at 0 ppm. Attempts to carry out ^{31}P MASNMR spectroscopy on other samples of copper, mixed copper–zinc vinylphosphonates and their intercalated compounds have not given any useful information, owing to the paramagnetic nature of Cu^{II}.

Preparation of copper–zinc oxide precursors: The range of copper–zinc oxides ($Cu^{II}_{1-x}Zn^{II}_xO$) with different ratios of zinc content ($x = Zn/(Cu + Zn) = 0, 0.1, 0.25, 0.5, 1$) was obtained by the following standard procedure.

A solution (0.04 M in metal, 100 mL), containing copper(II) nitrate hemipentahydrate $Cu^{II}(NO_3)_2 \cdot 2.5\,H_2O$ ($0.04(1-x)$ mol) and zinc nitrate hexahydrate $Zn^{II}(NO_3)_2 \cdot 6\,H_2O$ ($0.04(x)$ mol) in distilled water was slowly dropped, with stirring, into sodium hydroxide solution (0.4 M, 100 mL). Upon completion of addition, the mixture was heated under reflux for 6 h. The precipitates formed for the pure copper oxide (black powder), mixed divalent copper–zinc oxides (brownish) and zinc oxide (colourless) were then filtered, washed thoroughly with distilled water until neutral pH and dried overnight in the oven at 60 °C.

Preparation of copper–zinc vinylphosphonates $Cu^{II}_{1-x}Zn^{II}_x(O_3PC_2H_3)\cdot H_2O$: Copper–zinc vinylphosphonate materials, $Cu^{II}_{1-x}Zn^{II}_x(O_3PC_2H_3)\cdot H_2O$ (with $x = 0$, 0.1, 0.25, 0.5, 1) were obtained by mixing the corresponding copper–zinc oxides $Cu^{II}_{1-x}Zn^{II}_xO$ (5 mmol, 1 equiv) together with an excess quantity of the relevant vinylphosphonic acid $H_2PO_3C_2H_3$ (6 mmol, 1.2 equiv). The mixtures were ground and placed in an autoclave and heated for four days at 105 °C (which is above the melting point of the vinylphosphonic acid of 45 °C). The resulting brown-green solid compounds were washed with distilled water and acetone, to remove any unreacted vinylphosphonic acid, recovered by filtration and dried overnight in the oven at 60 °C. The typical yield was approximately 90% for all the series.

Pure copper vinylphosphonate and zinc vinylphosphonate could also be obtained by the coprecipitation method from a range of metal precursors: the desired metal oxide or hydroxide (e.g., $Cu^{II}O$, $Zn^{II}O$, $Cu^{II}(OH)_2$, $Zn^{II}(OH)_2$) or the corresponding metal nitrate ($Cu^{II}(NO_3)_2 \cdot 2.5\,H_2O$, $Zn^{II}(NO_3)_2 \cdot 6\,H_2O$, 10 mmol) with an excess of the corresponding vinylphosphonic acid (13 mmol) were dissolved in distilled water (25 mL), and urea (40 mmol) was added before heating overnight at 80 °C. Upon filtering, copper vinylphosphonate was obtained as blue, plate crystals and zinc vinylphosphonates as fine, colourless crystals. Characterisation by powder X-ray diffraction confirmed that the structures were the same for all the compounds prepared by different methods and precursors.

Elemental analyses of these samples (for C and H) and thermogravimetric analysis data are in good agreement with the proposed formulations, as shown below for $Cu^{II}_{1-x}Zn^{II}_x(O_3PC_2H_3)\cdot H_2O$.

$Cu(O_3PC_2H_3)\cdot H_2O$: Elemental analysis calcd (%) for $C_2H_5O_4PCu$ (186.92): C 12.83, H 2.67; found C 12.79, H 2.61; TGA (water loss) calcd (%): 9.62; found 9.7.

$Cu_{0.9}Zn_{0.1}(O_3PC_2H_3)\cdot H_2O$: Elemental analysis calcd (%) for $C_2H_5O_4PCu_{0.9}Zn_{0.1}$ (187.69): C 12.78, H 2.66; found C 12.95, H 2.48; TGA (water loss) calcd (%): 9.59; found 9.3.

$Cu_{0.75}Zn_{0.25}(O_3PC_2H_3)\cdot H_2O$: Elemental analysis calcd (%) for $C_2H_5O_4PCu_{0.75}Zn_{0.25}$ (187.96): C 12.76, H 2.68; found C, 12.88; H, 2.57%; TGA (water loss) calcd (%): 9.57; found 9.1.

$Cu_{0.5}Zn_{0.5}(O_3PC_2H_3)\cdot H_2O$: Elemental analysis calcd (%) for $C_2H_5O_4PCu_{0.5}Zn_{0.5}$ (188.42): C 12.73, H 2.65; found C 12.86, H 2.75; TGA (water loss) calcd (%): 9.55; found 9.0.

$Zn(O_3PC_2H_3)\cdot H_2O$: Elemental analysis calcd (%) for $C_2H_5O_4PZn$ (189.42): C 12.68, H 2.66; found C 12.65, H 2.62; TGA (water loss) calcd (%): 9.50; found 9.4.

Dehydration and intercalation of $Cu^{II}_{1-x}Zn^{II}_x(O_3PC_2H_3)\cdot H_2O$ with *n*-butylamine: The dehydration of the range of copper–zinc vinylphosphonates, $Cu^{II}_{1-x}Zn^{II}_x(O_3PC_2H_3)\cdot H_2O$ ($x = 0$, 0.1, 0.25, 0.5 and 1, 0.2 g), was carried out by heating the monohydrate under vacuum at 180 °C overnight in a Schlenk tube. The resulting dehydrates were pale blue (for pure copper vinylphosphonate), grey (for phosphonates obtained by copper–zinc oxides precursors by the autoclave method) or white (pure zinc vinylphosphonate).

Dehydrated compounds were subsequently placed under nitrogen at room temperature, and neat *n*-butylamine (15 mL) was added to give intercalated copper–zinc vinylphosphonates. Upon contact with the amine, the solids changed from their dehydrated colour to a dark blue in all cases except for that of zinc vinylphosphonate, which remained colourless. These sealed tubes were held under these conditions for one week, with stirring, before filtering off of the product.

Elemental analyses of the samples for C, H and N are in good agreement with the proposed formulations, as shown below for $Cu^{II}_{1-x}Zn^{II}_x(O_3PC_2H_3)\cdot[(C_4H_9NH_2)_{1-x}(C_4H_9NH_2)_x]_2$ and $Zn^{II}(O_3PC_2H_3)\cdot(C_4H_9NH_2)$.

$Cu(O_3PC_2H_3)\cdot[C_4H_9NH_2]_2$: Elemental analysis calcd (%) for $C_{10}H_{25}O_3PN_2Cu$ (315.84): C 38.03, H 7.98, N 8.87; found C 37.85, H 7.70, N 8.65.

$Cu_{0.9}Zn_{0.1}(O_3PC_2H_3)\cdot[C_4H_9NH_2]_2$: Elemental analysis calcd (%) for $C_{10}H_{25}O_3PN_2Cu_{0.9}Zn_{0.1}$ (316.02): C 37.97, H 7.91, N 8.86; found C 37.77, H 7.81, N 8.68.

$Cu_{0.75}Zn_{0.25}(O_3PC_2H_3)\cdot[C_4H_9NH_2]_2$: Elemental analysis calcd (%) for $C_{10}H_{25}O_3PN_2Cu_{0.75}Zn_{0.25}$ (316.29): C 37.94, H 7.90, N 8.85; found C 37.66, H 7.68, N 8.61.

$Cu_{0.5}Zn_{0.5}(O_3PC_2H_3)\cdot[C_4H_9NH_2]_2$: Elemental analysis calcd (%) for $C_{10}H_{25}O_3PN_2Cu_{0.5}Zn_{0.5}$ (316.76): C 37.88, H 7.89, N 8.83; found C 37.53, H 7.90, N 8.39.

$Zn(O_3PC_2H_3)\cdot(C_4H_9NH_2)$: Elemental analysis calcd (%) for $C_6H_{14}O_3PNZn$ (244.54): C 29.47, H 5.77, N 5.73; found C 29.44, H 5.75, N, 5.42.

Acknowledgements

We would like to acknowledge the EPSRC for support (Research grant to BM). We wish to thank Dr. J. A. Hriljac for assistance with the D5005 diffractometer for the powder X-ray patterns recorded at high temperature, Dr S. J. Kitchin for help in collecting the solid-state NMR data, and L. Hill for carrying out the CHN elemental analysis.

[1] A. Clearfield in *Progress in Inorganic Chemistry*, *Vol. 47* (Ed. K. D. Karlin), Wiley, New York, **1998**, pp. 371–510.
[2] G. Alberti, M. Casciola, U. Costantino, R. Vivani, *Adv. Mater.* **1996**, *8*, 291–303.
[3] A. Clearfield, U. Costantino in *Comprehensive Supramolecular Chemistry*, *Vol. 7* (Ed. G. Alberti, T. Bein), Pergamon, Oxford, **1996**, pp. 107–149.
[4] D. M. Poojary, H. L. Hu, F. L. Campbell, A. Clearfield, *Acta Crystallogr. Sect* B **1993**, *49*, 996–1001.
[5] G. Cao, H. Lee, V. M. Lynch, T. E. Mallouk, *Inorg. Chem.* **1988**, *27*, 2781–2785.
[6] G. B. Hix, K. D. M. Harris, *J. Mater. Chem.* **1998**, *8*, 579–584.
[7] G. Cao, H. Lee, V. M. Lynch, T. E. Mallouk, *Solid State Ionics* **1988**, *26*, 63–69.
[8] K. J. Martin, P. J. Squattrito, A. Clearfield, *Inorg. Chim. Acta* **1989**, *155*, 7–9.
[9] L. Raki, C. Detellier, *Chem. Commun.* **1996**, 2475–2476.
[10] A. Cabeza, M. A. G. Aranda, S. Bruque, D. M. Poojary, A. Clearfield, *Mater. Res. Bull.* **1998**, *33*, 1265–1274.
[11] J. Lebideau, B. Bujoli, A. Jouanneaux, C. Payen, P. Palvadeau, J. Rouxel, *Inorg. Chem.* **1993**, *32*, 4617–4620.
[12] P. Gerbier, C. Guerin, B. Henner, J.-R. Unal, *J. Mater. Chem.* **1999**, *9*, 2559–2565.
[13] J. Lebideau, C. Payen, P. Palvadeau, B. Bujoli, *Inorg. Chem.* **1994**, *33*, 4885–4890; B. Bujoli, O. Pena, P. Palvadeau, J. Lebideau, C. Payen, J. Rouxel, *Chem. Mater.* **1993**, *5*, 583–587.
[14] G. Alberti, U. Costantino, M. Casciola, R. Vivani, A. Peraio, *Solid State Ionics* **1991**, *46*, 61–68.
[15] S. Drumel, P. Janvier, P. Barboux, M. Bujoli-Doeuff, B. Bujoli, *Inorg. Chem.* **1995**, *34*, 148–156.
[16] P. M. Di Giacomo, M. B. Dines, *Polyhedron* **1982**, *1*, 61–68.
[17] C.-Y. Yang, A. Clearfield, *React. Polym.* **1987**, *5*, 13–21.
[18] S. J. Hartman, E. Todorov, C. Cruz, S. C. Sevov, *Chem. Commun.* **2000**, 1213–1214.
[19] G. Alberti, F. Marmottini, S. Murcia-Mascaros, R. Vivani, *Angew. Chem.* **1994**, *106*, 1655–1658; *Angew. Chem. Int. Ed. Engl.* **1994**, *33*, 1594–1597.
[20] V. V. Krishnan, A. G. Dokoutchaev, M. E. Thompson, *J. Catal.* **2000**, *196*, 366–374.
[21] B. L. Zhang, A. Clearfield, *J. Am. Chem. Soc.* **1997**, *119*, 2751–2752.
[22] D. M. Poojary, A. Clearfield, *J. Am. Chem. Soc.* **1995**, *117*, 11278–11284.
[23] G. Cao, T. E. Mallouk, *Inorg. Chem.* **1991**, *30*, 1434–1438.
[24] Y.-P. Zhang, K. J. Scott, A. Clearfield, *Chem. Mater.* **1993**, *5*, 495–499.

  0947-6539/02/0821-4892 $ 20.00+.50/0

[25] J. W. Johnson, A. J. Jacobson, W. M. Butler, S. E. Rosenthal, J. F. Brody, J. T. Lewandowski, *J. Am. Chem. Soc.* **1989**, *111*, 381–383.
[26] P. A. Wright, R. H. Jones, S. Natarajan, R. G. Bell, J. Chen, M. B. Hursthouse, J. M. Thomas, *J. Chem. Soc. Chem. Commun.* **1993**, 633–635.
[27] G. Alberti, U. Costantino, C. Dionigi, S. Murcia-Mascaros, R. Vivani, *Supramol. Chem.* **1995**, *6*, 29–40.
[28] A. Clearfield, *Chem. Mater.* **1998**, *10*, 2801–2810.
[29] G. B. Hix, B. M. Kariuki, S. Kitchin, M. Tremayne, *Inorg. Chem.* **2001**, *40*, 1477–1481.
[30] D. Cunningham, P. J. D. Hennelly, T. Deeney, *Inorg. Chim. Acta* **1979**, *37*, 95–102.
[31] Y.-P. Zhang, A. Clearfield, *Inorg. Chem.*, **1992**, *31*, 2821–2826.
[32] B. Menaa, B. M. Kariuki, I. J. Shannon, *New J. Chem.* **2002**, *26*, 906–909.
[33] M. J. Vela, V. Buchholz, V. Enkelmann, B. B. Snider, B. M. Foxman, *Chem. Commun.* **2000**, 2225–2226.
[34] F. L. Hirschfeld, G. M. J. Schmidt, *J. Polym. Sci. Sect. A* **1964**, *2*, 2181–2190.
[35] B. Menaa, I. J. Shannon, *J. Mater. Chem.* **2002**, *12*, 350–355.
[36] M. Bujoli-Doeuff, M. Evain, P.-A. Jaffres, V. Caignaert, B. Bujoli, *Int. J. Inorg. Mater.* **2000**, *2*, 557–560.
[37] Y.-P. Zhang, K. J. Scott, A. Clearfield, *J. Mater. Chem.* **1995**, *5*, 315–318.
[38] S. Drumel, P. Janvier, M. Bujoli-Doeuff, B. Bujoli, *J. Mater. Chem.* **1996**, *6*, 1843–1847.
[39] G. Cao, V. M. Lynch, L. N. Yacullo, *Chem. Mater.* **1993**, *5*, 1000–1006.

Received: April 26, 2002 [F4057]

  0947-6539/02/0821-4893 $ 20.00+.50/0